Thermophysical investigation of glycol ethers in mannitol solutions at various temperatures

NABAPARNA CHAKRABORTY[1,2*], PRIYA THAKUR[1], KAILASH CHANDRA JUGLAN[1] and ABRAR HUSSAIN SYED[3]

[1]*Department of Physics, Lovely Professional University, Phagwara, 144401, Punjab, India,* [2]*Central Instrumentation Facility, Research and Development Cell, Lovely Professional University, Phagwara, 144401, Punjab, India and* [3]*Research and Development, Saputo Dairy Australia, Freshwater Place, 3006, Victoria, Australia*

Abstract: Ultrasonic analysis can be very helpful to comprehend the molecular dynamics and interactions in liquid systems. Employing the Anton-Paar (DSA 5000 M) at concentrations and 0.1 MPa, sound speed as well as density of glycol ethers, *i.e.*, phenoxyethanol (PE) and butoxyethanol (BE) in solutions of a well-known sugar alcohol (D-mannitol), were measured at 288.15–303.15 K. A variety of advanced acoustic-thermodynamic parameters, including apparent molar parameters, partial molar parameters and transfer molar properties, were estimated using the experimentally attained the velocity and density values. These derived values are used to express the interactions between solutes and their solvents. The propensity of the solute to generate or destroy structures in a solvent is also a subject of research. Analysis was done on the interactions between the molecules in the ternary mixture of D-mannitol and glycol ethers in aqueous medium.

Keywords: phenoxyethanol; butoxyethanol; kosmotropes; chaotropic; acoustic and volumetric.

INTRODUCTION

Every industry has recognized the usage of chemicals. By examining the physicochemical characteristics of diverse liquids and mixtures using ultrasonic techniques, numerous studies into the molecular interactions have been conducted. The pharmaceutical, healthcare, cosmetic, food, leather, textile and automotive industries all heavily rely on the use of ultrasonic technology to characterize various thermophysical properties of liquid mixtures as well as their behavior. Details about the character and intensity of molecular interactions occurring within the mixture, is obtained from this technique since it is a non-destructive

for describing the liquid systems.[1–4] The binding forces that form between the molecules in a liquid directly affect the ultrasonic speed at which sound travels through it.[5–9]

Phenoxyethanol, commonly known as 2-phenoxyethanol, is an aromatic alcohol that is colorless and has a pleasant smell. Phenoxyethanol serves as an antibacterial and is a common preservative in cosmetic goods. It works well against a variety of bacteria and yeasts. The US Food and Drug Administration has given 2-butoxyethanol permission for use as an adhesive, antibacterial agent, defoamer, stabilizer, and preservative in food additives.[9–12]

Mannitol is a sugar alcohol or polyol with the chemical formula $C_6H_{12}O_6$ that is used as a sweetener and in medicine. Mannitol is a member of the class of medications known as diuretics. D-Mannitol is readily available, reasonably priced, and available in a variety of granular and powder forms. Water molecules interact hydrophilically with mannitol. Due to the creation of H-bonds, D-mannitol and water molecules become associated molecularly. It is critically important for biological reasons because polyhydroxy chemicals assist stabilize globular proteins.[13–17]

Glycol ethers (PE/BE) have been the subject of extensive research, for instance, Scognamiglio *et al*. had analysed the toxic and dermatological behaveiour of phenoxyethanol, which finds application as an ingredient in fragrances.[18] Whereas, Lowe and Southern had investigated the antibacterial properties of phenoxyethanol and thiomersal, two preservatives.[19] Both substances demonstrated equal effectiveness at inactivating challenge doses of yeast, Gram-positive and Gram-negative microorganisms, and reported that phenoxyethanol had no effect on Gram-positive bacteria, but the yeast and both Gram-positive challenge strains were rendered inactive by the vaccines as they were created.

Raman *et al*. had studied the intermolecular association in aqueous mannitol solutions at multiple temperatures by evaluating various thermo-acoustic parameters from the experimental values of density and velocity. These properties advocate the strong molecular interlinkage in the system.[20]

The literature review on mannitol and glycol ethers indicates that no volumetric and acoustic investigations for their combination have been published yet. Based on the experimental findings, several thermodynamic parameters were calculated to uncover the physical and chemical characteristics of the liquid system. Glycol ethers and mannitol are commonly utilized in industries such as medicine, cosmetics and chemicals. This present study aims to elucidate the intermolecular interactions occurring in liquid mixtures, providing an opportunity to assess the mixture and explore different attributes and properties that enhance the quality of the product.

EXPERIMENTAL

Materials used

Phenoxyethanol, butoxyethanol and D-mannitol are the chemicals employed in the current experiment; their molar masses are 118.16, 138.16, and 182.172 g·mol^{-1}, respectively. The solvent mixtures were made using the sugar alcohol D-mannitol and degassed, triple-distilled water. Table I presents the characteristics of the compounds utilized in the study. The mass fraction purities of, PE, BE and D-mannitol are all greater than 0.99. Although the chemicals were dried and stored in desiccators over P_2O_5 for two days before usage, they were employed without additional purification.

Methods used

The Anton-Paar DSA 5000 M instrument provides a reliable and accurate data for the density and speed of sound. The high level of precision and accuracy required in the measurements is crucial to ensure the validity of the results. The obtained measurements of different concentration calculation methods that are included into the DSA use density and sound speed as inputs. Degassed, triple-distilled water with a specific conductance of less than 10^{-6} S·cm^{-1} was used to create the solutions. The Sartorius CPA 225D was used to weigh the samples and the precision was within ±0.00001 g. The density and sound speed measurements have precisions of ±0.001 kg·m^{-3} and ±0.01 m·s^{-1}, respectively. The corresponding measurement uncertainties were ±0.001 K, ±0.15 kg·m^{-3} and ±0.01 m·s^{-1}, respectively for temperature, density and speed of sound.

TABLE I. Specifications of the chemicals utilized in this present investigation

Chemical	Butoxyethanol	Phenoxyethanol	D-Mannitol
Source	Loba Chemie Pvt. Ltd., India		Sigma–Aldrich
Mass fraction purity (supplier)	≥0.99	≥0.99	≥0.99
Purification method	Used as such	Used as such	Used as such

RESULTS AND DISCUSSION

Density

Experimental density values (ρ) for butoxyethanol (BE) and phenoxyethanol (PE) in aqueous solutions of mannitol with 0.00, 0.02, 0.06 and 0.1 mol·kg^{-1} concentrations, were obtained at temperatures of 288.15–303.15 K and 0.1 MPa pressure. The experimental density values for (water + mannitol) were cross-referenced with values from literature at 288.15, 293.15, 298.15 and 303.15 K, which is shown in Fig. 1a, and the consistency between the experimental results and the values found in the literature is demonstrated.[21,22] For this binary system, Fig. 2 plots the deviation in density between the experimental density values and those reported[21,22] at 288.15, 293.15, 298.15 and 303.15 K. It finds a good agreement, with the maximum deviation falling within the reported experimental error.

By measuring the density of pure components, each experimental chemical used in this work was verified, and the data were compared to the values found in the literature,[23,24] which are listed in Table II along with the percentage deviation between the data from the experiment and reported data. In Table III the

density values of glycol ethers at a specific concentration of mannitol are recorded, and it can be observed that the ρ values are exhibiting linear trend, *i.e.*, increasing with the rising values of mannitol concentrations as well as with the molality of glycol ethers. This behavior implies that the water molecules form a new structure, in existence that is more when projecting at higher concentrations. The decline in ρ values occurs when the kinetic energy of solution molecules exceeds the binding energy at high temperatures.[25–27] Overall, the study provides a comprehensive analysis of the density values of BE and PE in mannitol solutions at different temperatures and mannitol concentrations in aqueous medium.[28,29]
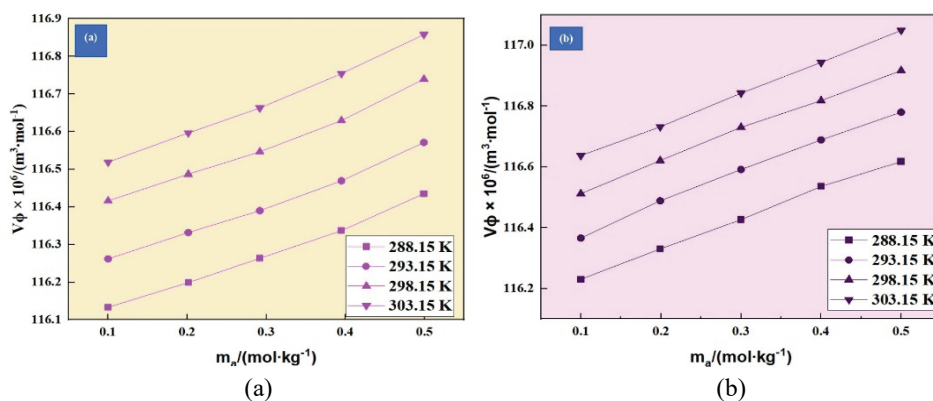

Fig. 1. The comparison graph between the experimental and literature[21,22] values for:
a) density and b) speed of sound for the binary solution of (D-mannitol + water)
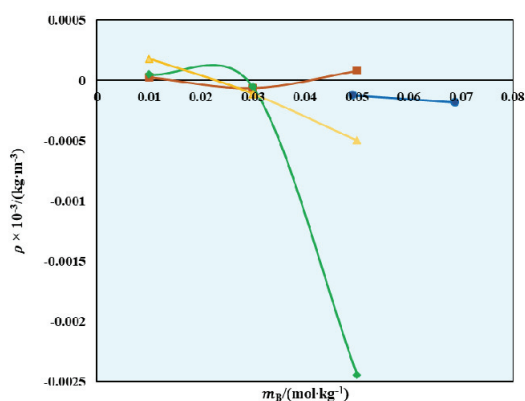at different temperatures against molality of D-mannitol.

Fig. 2. Plot of deviation in densities, ρ, of binary mixture (D-Mannitol + water) with the literature data at different temperatures; circle-blue: 288.15 K[22]; square-brown: 293.15 K[21], diamond-green: 298.15 K[21], triangle-yellow: 303.15 K[21].

Speed of sound

For the binary system of (water + mannitol), Fig. 3 plots the deviation in speed of sound between the experimental and literature[21,22] at 293.15, 298.15 and 303.15 K. It reaches a satisfactory agreement, with the highest difference fall-

TABLE II. Comparison of experimental densities (ρ) and ultrasonic velocities (v) with literature values for pure chemicals at different temperatures

Chemical	T / K	$\rho \times 10^{-3}$ / kg·m^{-3}			v / m·s^{-1}		
		Exp.	Lit.	% Deviation	Exp.	Lit.	% Deviation
Butoxyethanol	288.15	0.9032	–	–	1341.04	–	–
(BE)	293.15	0.9001	0.9001[23]	0.00000	1322.45	1322.50[23]	0.00378
	298.15	0.8960	0.8959[23]	0.01116	1305.06	1304.94[23]	0.03218
	303.15	0.8917	0. 8917[23]	0.00000	1288.52	1288.02[23]	0.03
Phenoxyethanol	288.15	1.1150	–	–	1608.56	–	–
(PE)	293.15	1.1080	1.1070[24]	0.09033	1592.00	1591.80[24]	0.0020
	298.15	1.1020	1.1030[24]	0.09066	1575.02	1574.60[24]	0.0042
	303.15	1.0970	1.0990[24]	0.18198	1557.80	1557.40[24]	0.0040

TABLE III. Values of density (ρ / g·cm^{-3}) of (BE/PE) in aqueous solutions of D-mannitol at different temperatures 288.15–303.15 K; m_a is the molality of glycols in the aqueous solution D-mannitol, standard uncertainties, u, are $u(m) = 1$ %, $u(T) = 0.001$ K and $u(\rho) = 0.15$ kg·m^{-3}

m_a	T / K				m_a	T / K			
	288.15	293.15	298.15	303.15		288.15	293.15	298.15	303.15
mol·kg^{-1}	0.00 mol·kg^{-1} D-mannitol + BE				mol·kg^{-1}	0.02 mol·kg^{-1} D-mannitol + BE			
0.00000	0.9992	0.9982	0.9970	0.9956	0.00000	1.0006	0.9997	0.9984	0.9970
0.10016	0.9994	0.9984	0.9972	0.9958	0.09978	1.0008	0.9999	0.9986	0.9972
0.20147	0.9996	0.9986	0.9974	0.9960	0.19899	1.0009	1.0001	0.9988	0.9974
0.29196	0.9998	0.9987	0.9976	0.9962	0.30003	1.0011	1.0002	0.9989	0.9975
0.39510	0.9999	0.9989	0.9977	0.9963	0.40010	1.0012	1.0003	0.9990	0.9976
0.49928	1.0001	0.9990	0.9978	0.9965	0.50003	1.0013	1.0004	0.9991	0.9977
	0.06 mol·kg^{-1} D-mannitol + BE					0.1 mol·kg^{-1} D-mannitol + BE			
0.00000	1.0031	1.0021	1.0009	0.9996	0.00000	1.0056	1.0045	1.0034	1.0021
0.10034	1.0032	1.0023	1.0010	0.9998	0.09894	1.0057	1.0046	1.0035	1.0022
0.20009	1.0034	1.0024	1.0011	0.9999	0.19880	1.0058	1.0046	1.0035	1.0022
0.30012	1.0035	1.0025	1.0012	1.0000	0.30001	1.0058	1.0047	1.0036	1.0023
0.39990	1.003	1.0026	1.0013	1.0001	0.39959	1.0059	1.0047	1.0036	1.0024
0.50023	1.003	1.0026	1.0014	1.0001	0.50005	1.0059	1.0048	1.0037	1.0024
	0.00 mol·kg^{-1} D-mannitol + PE					0.02 mol·kg^{-1} D-mannitol + PE			
0.00000	0.9992	0.9982	0.9970	0.9956	0.00000	1.0006	0.9997	0.9984	0.9970
0.09102	0.9996	0.9986	0.9974	0.9961	0.09983	1.0010	1.0002	0.9989	0.9975
0.20047	1.0002	0.9991	0.9979	0.9966	0.20034	1.0015	1.0006	0.9993	0.9979
0.29106	1.0005	0.9995	0.9983	0.9969	0.30010	1.0019	1.0010	0.9997	0.9983
0.39951	1.0009	0.9999	0.9987	0.9974	0.39990	1.0022	1.0014	1.0001	0.9987
0.49928	1.0013	1.0002	0.9991	0.9977	0.50004	1.0026	1.0017	1.0004	0.9991
	0.06 mol·kg^{-1} D-mannitol + PE					0.1 mol·kg^{-1} D-mannitol + PE			
0.00000	1.0031	1.0021	1.0009	0.9996	0.00000	1.0056	1.0045	1.0034	1.0021
0.10028	1.0035	1.0025	1.0013	1.0001	0.09999	1.0060	1.0049	1.0038	1.0025
0.19996	1.0039	1.0029	1.0017	1.0004	0.19973	1.0063	1.0052	1.0041	1.00282
0.30056	1.0042	1.0033	1.0020	1.0008	0.29880	1.0066	1.0055	1.0044	1.0031
0.40031	1.0045	1.0036	1.0023	1.0011	0.40050	1.0069	1.0058	1.0047	1.0034
0.50009	1.0048	1.0039	1.0027	1.0015	0.50009	1.0072	1.0061	1.0050	1.0037

ing within the expected experimental margin of error. The speed of sound of these chemicals used in this study was confirmed by measuring the speed of sound of pure components, and the results were compared to values from previous studies[23,24] listed in Table II, including the percentage difference between experimental and reported data. At 288.15–303.15 K, the speed of sound (v) of glycol ethers in aqueous mannitol solutions, at different temperatures (and mannitol concentrations 0.00, 0.02, 0.06 and 0.1 mol·kg^{-1}), are expressed in Table IV. For the experimentally acquired speed of sound values for (water + mannitol), a comparison was made between the obtained values and the values documented in the literature for at certain temperatures. The experimental v measurements align with the velocity values reported in the literature for various temperatures, as illustrated in Fig 1b.[21] Results showed that speed of sound values increased with temperature and (BE/PE) molality, and there was an observable rise in speed of sound with an increase in mannitol concentration, which can be attributed to the presence of a three-dimensional network of hydrogen bonds within the water structure. Intramolecular and intermolecular hydrogen bonds in solute–solvent molecules caused a hike in speed of sound values, while hydrogen bond formation between water and mannitol degraded with the acceleration in the molar mass of glycol ethers. The formation of a hydrogen bond network occurs between the solute and aqueous mannitol molecules resulted in a rise of speed of sound values with mannitol concentration, and new H-bonds were created between glycol ethers and mannitol molecules. The study provided a comprehensive analysis of factors influencing speed of sound values in glycol ethers in aqueous mannitol solutions at different temperatures and mannitol concentrations.[30–36]
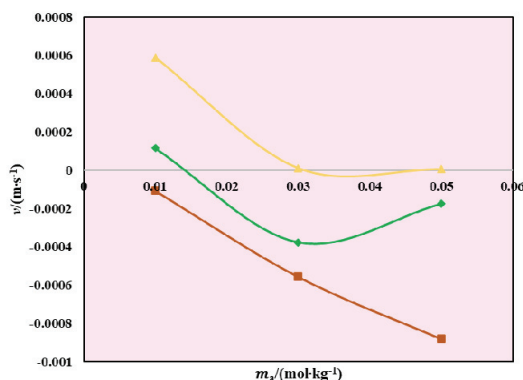

Fig. 3. Plot of deviation in speed of sound, v, of binary mixture (D-mannitol + water) with the literature data at different temperatures; square-brown: 293.15 K[21]; diamond-green: 298.15 K[21]; triangle-yellow: 303.15 K[21].

Apparent molar volume

The experimental density values were employed in the calculation of the apparent molar volume (V_Φ) for binary mixtures of glycol ethers (BE/PE) and

TABLE IV. Values of Speed of sound (v / m·s^{-1}) of BE/PE in aqueous solutions of D-mannitol at different temperatures 288.15–303.15 K; m_a is the molality of glycols in the aqueous solution D-mannitol, standard uncertainties, u, are $u(m)$ = 1 %, $u(T)$ = 0.001 K, u(v) = 1.0 m·s^{-1}

| m_a | T / K | | | | m_a | T / K | | | |
| | 288.15 | 293.15 | 298.15 | 303.15 | | 288.15 | 293.15 | 298.15 | 303.15 |
mol·kg^{-1}	0.00 mol·kg^{-1} D-mannitol + BE				mol·kg^{-1}	0.02 mol·kg^{-1} D-mannitol + BE			
0.00000	1466.6	1482.6	1495.9	1508.8	0.00000	1469.5	1485.1	1499.0	1511.4
0.10016	1467.6	1483.5	1497.0	1509.6	0.09978	1470.4	1485.9	1500.2	1512.2
0.20147	1468.6	1484.5	1498.2	1510.5	0.19899	1471.5	1486.8	1501.4	1513.1
0.29196	1469.5	1485.4	1499.5	1511.4	0.30003	1472.5	1487.9	1502.8	1514.0
0.39510	1470.9	1486.6	1501.0	1512.4	0.40010	1473.6	1488.9	1504.0	1515.1
0.49928	1472.1	1487.7	1502.6	1513.6	0.50003	1474.9	1489.9	1505.4	1516.2
	0.06 mol·kg^{-1} D-mannitol + BE					0.1 mol·kg^{-1} D-mannitol + BE			
0.00000	1473.4	1489.3	1503.1	1516.	0.00000	1476.8	1492.8	1507.4	1520.6
0.10034	1474.4	1490.2	1504.1	1516.8	0.09894	1477.8	1493.7	1508.4	1521.3
0.20009	1475.4	1491.0	1505.4	1517.7	0.19880	1478.8	1494.5	1509.6	1522.4
0.30012	1476.2	1492.0	1506.5	1518.5	0.30001	1479.7	1495.3	1510.7	1523.4
0.39990	1477.4	1492.9	1507.6	1519.6	0.39959	1480.8	1496.3	1511.7	1524.5
0.50023	1478.5	1493.8	1508.8	1520.7	0.50005	1481.9	1497.4	1512.8	1525.6
	0.00 mol·kg^{-1} D-mannitol + PE					0.02 mol·kg^{-1} D-mannitol + PE			
0.00000	1466.6	1482.6	1495.9	1508.8	0.00000	1469.5	1485.1	1499.0	1511.4
0.09102	1468.3	1484.2	1497.5	1510.5	0.09983	1471.2	1487.0	1500.6	1513.4
0.20047	1470.3	1486.3	1499.5	1512.7	0.20034	1473.1	1489.1	1502.6	1515.5
0.29106	1472.3	1488.2	1501.2	1514.4	0.30010	1475.3	1491.1	1504.4	1517.4
0.39951	1474.7	1490.3	1503.4	1516.5	0.39990	1477.6	1493.0	1506.7	1519.5
0.49928	1476.6	1492.2	1505.4	1518.6	0.50004	1479.5	1495.1	1508.8	1521.4
	0.06 mol·kg^{-1} D-mannitol + PE					0.1 mol·kg^{-1} D-mannitol + PE			
0.00000	1473.4	1489.3	1503.1	1516.0	0.00000	1476.8	1492.8	1507.4	1520.6
0.10028	1475.3	1491.0	1505.0	1518.0	0.09999	1478.7	1494.8	1509.2	1522.6
0.19996	1477.3	1493.1	157.02	1520.0	0.19973	1480.5	1496.8	1511.3	1524.5
0.30056	1479.4	1495.1	1509.1	1522.1	0.29880	1482.6	1498.8	1513.2	1526.5
0.40031	1481.5	1497.1	1511.0	1524.1	0.40050	1484.8	1500.8	1515.4	1528.5
0.50009	1483.5	1499.2	1513.0	1526.0	0.50009	1486.8	1502.8	1517.3	1530.6

mannitol. The equation used for this calculation included the densities of the solution (ρ) and solvent (ρ_0), the molality of the solute per kg of solvent (m_A), and molar mass (M) of the solute:

$$V_\Phi = M / \rho - (\rho - \rho_0) / m_A \rho \rho_0 \qquad (1)$$

Table V illustrates the positive values of V_Φ calculated for different mannitol concentrations and temperatures. As the temperature and mannitol concentration increased, the V_Φ values also increased. The observed increase in the apparent molar volume values with temperature implies a strong interaction between the solute and solvent in the mixture, as depicted in Fig. 4.[37–39] This suggests that

the solvent exhibits a higher affinity for the solute at elevated temperatures, leading to enhanced solute-solvent interactions.

TABLE V. Values of apparent molar volumes (V_Φ / m³·mol⁻¹) of BE/PE in aqueous solutions of D-mannitol at different temperatures 288.15–303.15 K; m_a is the molality of glycols in the aqueous solution D-mannitol, standard uncertainties, u, are $u(m)$ = 1 %, $u(T)$ = 0.001 K, $u(V_\Phi)$ = (0.023–0.028)×10⁶ m³ mol⁻¹

m_a mol·kg⁻¹	T / K				m_a mol·kg⁻¹	T / K			
	288.15	293.15	298.15	303.15		288.15	293.15	298.15	303.15
	0.00 mol·kg⁻¹ D-mannitol + BE					0.02 mol·kg⁻¹ D-mannitol + BE			
0.10016	116.13	116.26	116.42	116.52	0.09978	116.23	116.37	116.51	116.64
0.20147	116.20	116.33	116.49	116.60	0.19899	116.33	116.49	116.62	116.73
0.29196	116.26	116.39	116.55	116.66	0.30003	116.43	116.59	116.73	116.84
0.39510	116.34	116.47	116.63	116.75	0.40010	116.54	116.69	116.82	116.94
0.49928	116.44	116.57	116.74	116.86	0.50003	116.62	116.78	116.92	117.05
0.10016	116.13	116.26	116.42	116.52	0.09978	116.23	116.37	116.51	116.64
	0.06 mol·kg⁻¹ D-mannitol + BE					0.1 mol·kg⁻¹ D-mannitol + BE			
0.10034	116.35	116.46	116.60	116.73	0.09894	116.43	116.56	116.69	116.81
0.20009	116.45	116.56	116.71	116.82	0.19880	116.54	116.67	116.81	116.91
0.30012	116.54	116.66	116.81	116.93	0.30001	116.64	116.78	116.92	117.02
0.39990	116.65	116.76	116.91	117.03	0.39959	116.74	116.88	117.01	117.12
0.50023	116.76	116.87	117.03	117.15	0.50005	116.84	116.97	117.11	117.22
0.10034	116.35	116.46	116.60	116.73	0.09894	116.43	116.56	116.69	116.81
	0.00 mol·kg⁻¹ D-mannitol + PE					0.02 mol·kg⁻¹ D-mannitol + PE			
0.10034	116.35	116.46	116.60	116.73	0.09894	116.43	116.56	116.69	116.81
0.20009	116.45	116.56	116.71	116.82	0.19880	116.54	116.67	116.81	116.91
0.30012	116.54	116.66	116.81	116.93	0.30001	116.64	116.78	116.92	117.02
0.39990	116.65	116.76	116.91	117.03	0.39959	116.74	116.88	117.01	117.12
0.50023	116.76	116.87	117.03	117.15	0.50005	116.84	116.97	117.11	117.22
0.10034	116.35	116.46	116.60	116.73	0.09894	116.43	116.56	116.69	116.81
	0.06 mol·kg⁻¹ D-mannitol + PE					0.1 mol·kg⁻¹ D-mannitol + PE			
0.10028	133.70	133.78	133.88	133.96	0.09999	133.82	133.89	133.98	134.09
0.19996	133.82	133.89	133.98	134.06	0.19973	133.91	133.98	134.07	134.18
0.30056	133.91	133.98	134.08	134.16	0.29880	134.00	134.07	134.16	134.27
0.40031	133.99	134.07	134.17	134.25	0.40050	134.08	134.17	134.26	134.37
0.50009	134.09	134.17	134.27	134.35	0.50009	134.18	134.26	134.36	134.48
0.10028	133.70	133.78	133.88	133.96	0.09999	133.82	133.89	133.98	134.09

Corresponding to the co-sphere overlapping model, when ionic species interact in solutions, the volume of the solution increases, indicating the presence of molecular interactions within the system through the formation of cavities among the solution molecules.[4,5] These cavities expand as the temperature rises, facilitating the interaction between solute and solvent molecules. However, at lower temperatures, solute molecules encounter difficulties in fitting into the water structure, resulting in stronger interactions between solute and solvent molecules in solutions.[40–42] Similarly, at higher mannitol concentrations, more solute–solvent
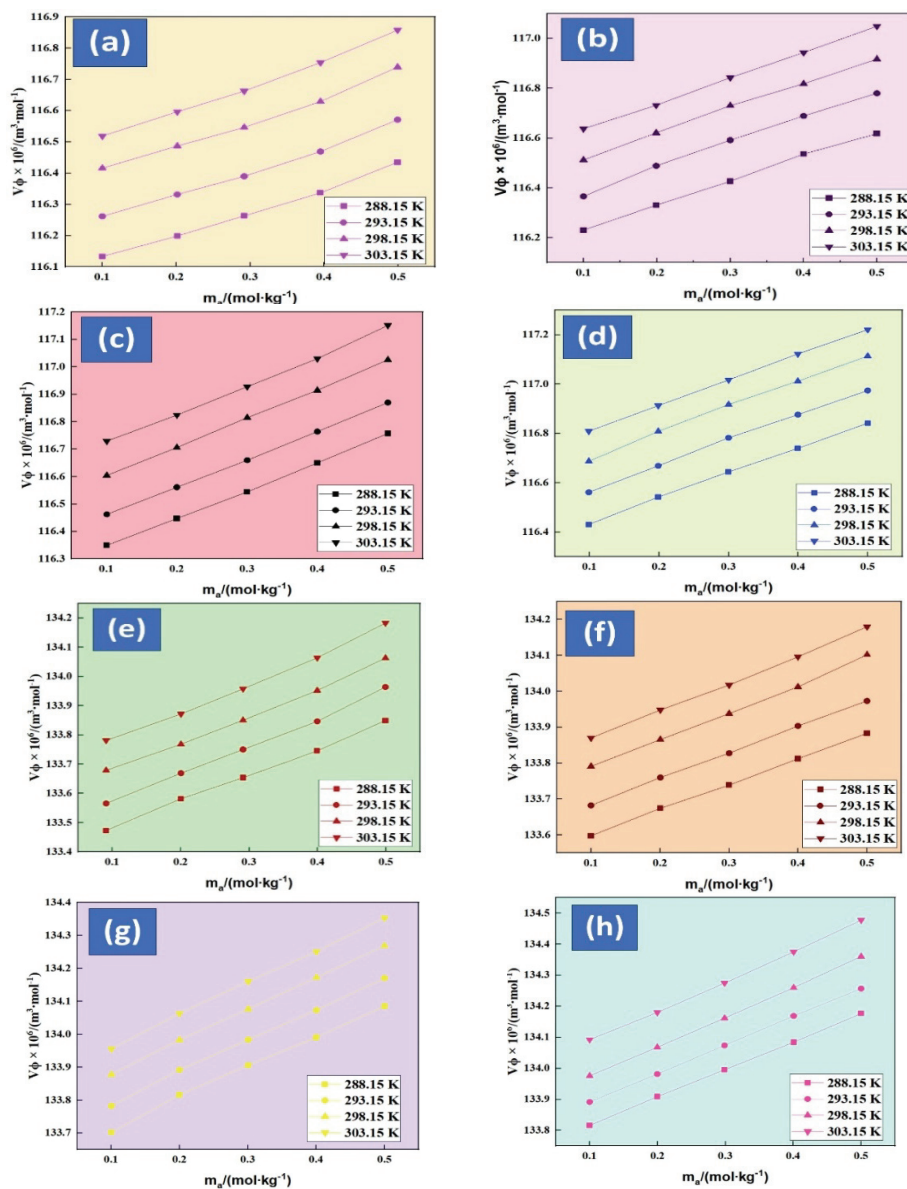
Fig. 4. Graphical illustration of apparent molar volume (V_Φ) against the molality of BE/PE (m_A) at different temperatures: a) 0.00 D-mannitol + BE + water, b) 0.02 D-mannitol + BE + water), c) 0.06 D-mannitol + BE + water, d) 0.1 D-mannitol + BE + water, e) 0.00 D-mannitol + PE + water, f) 0.02 D-mannitol + PE + water, (g) (0.06 D-mannitol + PE + water and h) 0.1 D-mannitol + PE + water.

interactions can occur as water constituents are held in place by strong hydrogen bonds instead of being directly attached to the surfaces of solute molecules. This leads to the formation of gaps or cavities in the solutions, consequently increasing the apparent molar volume.[40]

Moreover, the presence of glycol ethers in the mixture with water induces a combination of inter- and intramolecular hydrogen bonding, hydrophobic hydration, and dipole–dipole as well as dipole–induced dipole interactions.[21–23] The increase in solute–solvent interactions in the sample compositions, as the molar mass of glycol ethers increases from BE to PE, corresponds to the phenomenon of solvation in the mixture at high temperatures and a greater affinity of the solvent as depicted in the Scheme 1.[6–8]
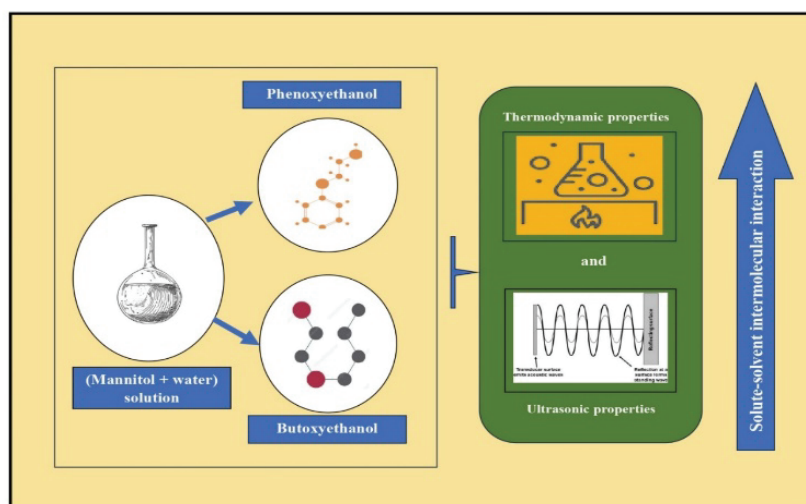
Scheme 1. Representation of BE/PE and mannitol interactions.

Apparent molar isentropic compressibility

The undermentioned formula is utilized to determine the isentropic compressibility of glycol ethers in aqueous mannitol solutions:

$$K_{\Phi,S} = (M k_S / \rho) - \{(k_{S,0}\rho - k_{S,0}\rho_0) / m_A \rho \rho_0\} \qquad (2)$$

which takes into account various parameters such as densities of solution (ρ) and solvent (ρ_0), molar mass of solute (M), molality of solute (m_A), and isentropic compressibility of pure solvent ($k_{S,O}$) and solution (k_S).

The following Laplace–Newton formula is used to compute the isentropic compressibility:[8]

$$k_S = 1 / v^2 \rho \qquad (3)$$

The values of apparent molar isentropic compressibility ($K_{\Phi,S}$) are presented in Table VI, depicting their variation with temperature, glycol ethers molality, and mannitol concentration. These relationships are also visually represented in Fig. 5. The negative values of $K_{\Phi,S}$ decrease as temperature and mannitol concentration increase, but they increase with higher glycol ethers molality. This behavior can be attributed to the expulsion of solute molecules by thermal agitation, leading to volume expansion and an increase in compressibility. The negative values indicate that water molecules near the ionic charge groups of glycol ethers are more compressible than the solute molecules, resulting in a reduction in the structural compressibility of water.[6–10] The presence of charged particles, such as ions, contributes to the overall rigidity of the solution, explaining the negative values of apparent molar isentropic compressibility in the presence of glycol ethers. As the temperature of the solution rises, the solution becomes more compressible due to the faster movement of ions and solvent molecules, which overcomes the resistance of the charged particles, resulting in enhanced compressibility.[10–13] The intermolecular hydrogen bonding between glycol ethers and mannitol molecules forms compact structures, contributing to the reduction in compressibility. Additionally, as compressibility increases at higher temperatures, the average distance between molecules increases. The significant solvent––solvent interactions are evident through the dipole–dipole interactions between nearby water molecules and the –OH groups of glycol ethers.[12–14]

TABLE VI. Values of apparent molar isentropic compressibility ($K_{\Phi} \times 10^6$ / m³ mol⁻¹ GPa⁻¹) of BE/PE in aqueous solutions of D-mannitol at different temperatures 288.15–303.15 K; m_a is the molality of glycols in the aqueous solution D-mannitol, standard uncertainties, u, are $u(m)$ = 1 %, $u(T)$ = 0.001 K, $u(K_{\Phi})$ = 0.11×10⁶ m³·mol⁻¹·GPa⁻¹

m_a	T / K				m_a	T / K			
	288.15	293.15	298.15	303.15		288.15	293.15	298.15	303.15
mol·kg⁻¹	0.00 mol·kg⁻¹ D-mannitol + BE				mol·kg⁻¹	0.02 mol·kg⁻¹ D-mannitol + BE			
0.10016	–46.04	–45.05	–44.25	–43.49	0.09978	–45.85	–44.90	–44.06	–43.34
0.20147	–46.28	–45.28	–44.48	–43.72	0.19899	–46.09	–45.13	–44.29	–43.57
0.29196	–46.36	–45.36	–44.56	–43.80	0.30003	–46.18	–45.21	–44.37	–43.65
0.39510	–46.41	–45.41	–44.60	–43.85	0.40010	–46.22	–45.26	–44.42	–43.69
0.49928	–46.44	–45.44	–44.63	–43.87	0.50003	–46.25	–45.28	–44.44	–43.72
0.10016	–46.04	–45.05	–44.25	–43.49	0.09978	–45.85	–44.90	–44.06	–43.34
	0.06 mol·kg⁻¹ D-mannitol + BE					0.1 mol·kg⁻¹ D-mannitol + BE			
0.10034	–45.61	–44.64	–43.83	–43.08	0.09894	–45.40	–44.43	–43.57	–42.82
0.20009	–45.85	–44.87	–44.06	–43.31	0.19880	–45.63	–44.66	–43.80	–43.04
0.30012	–45.93	–44.95	–44.13	–43.38	0.30001	–45.71	–44.74	–43.87	–43.12
0.39990	–45.97	–44.99	–44.17	–43.42	0.39959	–45.75	–44.78	–43.91	–43.16
0.50023	–45.99	–45.02	–44.20	–43.45	0.50005	–45.78	–44.80	–43.94	–43.18
0.10034	–45.61	–44.64	–43.83	–43.08	0.09894	–45.40	–44.43	–43.57	–42.82

TABLE VI. Continued

| m_a mol·kg^{-1}	*T* / K				m_a mol·kg^{-1}	*T* / K			
	288.15	293.15	298.15	303.15		288.15	293.15	298.15	303.15
0.00 mol·kg^{-1} D-mannitol + PE					0.02 mol·kg^{-1} D-mannitol + PE				
0.09102	−46.00	−45.01	−44.21	−43.46	0.09983	−45.87	−44.91	−44.08	−43.35
0.20047	−46.30	−45.31	−44.50	−43.75	0.20034	−46.12	−45.16	−44.32	−43.60
0.29106	−46.39	−45.40	−44.59	−43.83	0.30010	−46.21	−45.25	−44.41	−43.69
0.39951	−46.46	−45.46	−44.65	−43.89	0.39990	−46.27	−45.31	−44.47	−43.74
0.49928	−46.50	−45.50	−44.69	−43.93	0.50004	−46.31	−45.34	−44.50	−43.78
0.09102	−46.00	−45.01	−44.21	−43.46	0.09983	−45.87	−44.91	−44.08	−43.35
0.06 mol·kg^{-1} D-mannitol + PE					0.1 mol·kg^{-1} D-mannitol + PE				
0.10028	−45.63	−44.66	−43.84	−43.10	0.09999	−45.42	−44.45	−43.59	−42.84
0.19996	−45.87	−44.90	−44.08	−43.33	0.19973	−45.66	−44.68	−43.82	−43.07
0.30056	−45.96	−44.99	−44.17	−43.42	0.29880	−45.75	−44.77	−43.91	−43.15
0.40031	−46.02	−45.04	−44.22	−43.47	0.40050	−45.80	−44.82	−43.96	−43.20
0.50009	−46.05	−45.07	−44.26	−43.50	0.50009	−45.83	−44.86	−43.99	−43.23
0.10028	−45.63	−44.66	−43.84	−43.10	0.09999	−45.42	−44.45	−43.59	−42.84
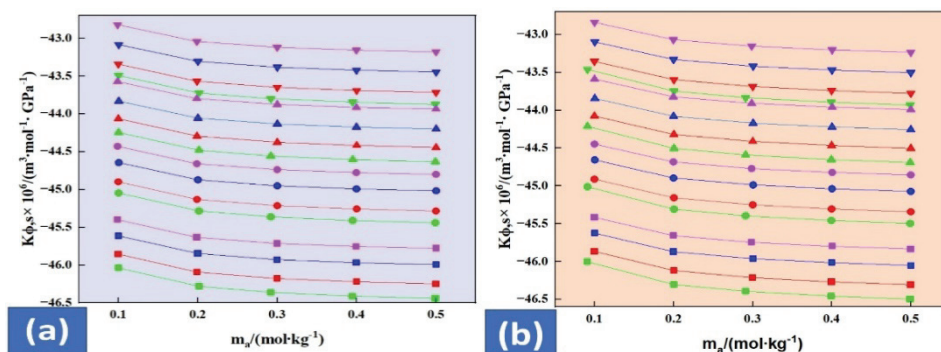
Fig. 5. Graphical illustration of apparent molar isentropic compressibility ($K_{\Phi,S}$), against the molality of BE/PE (m_A) at different temperatures: a) BE and b) PE (green, 0.00 D-mannitol; red, 0.02 D-mannitol; blue, 0.06 D-mannitol; purple, 0.1 D-mannitol; square, 288.15 K; circle, 293.15 K; triangle, 298.15 K; inverted triangle, 303.15 K).

Partial molar properties

Partial molar volume. The undermentioned formula used to attain the partial molar volume of solution containing mannitol and glycol ethers. The partial molar volume (V_Φ^0) values and experimental slope (S_V^*) along with their standard errors corresponding to experimental temperatures and mannitol concentrations, obtained using the least square fitting method, are demonstrated in Table VII. The equation used is:

$$V_\Phi = V_\Phi^0 + S_V^* m_A \tag{4}$$

The positive values of V_Φ^0 increase with the concentration of mannitol and temperature, indicating the solute-solvent interactions in the liquid mixture which is shown in Fig. 6. According to the co-sphere overlap model, the overlap of the hydration co-sphere between two ionic species results in an increase in volume, whereas the overlap of ion–hydrophobic and hydrophobic–hydrophobic groups leads to a decrease in volume.[4,5] Thus, the positive values of V_Φ^0 indicate that ion–hydrophilic interactions prevail over hydrophobic–hydrophobic and ion––hydrophobic interactions, providing evidence for the strong hydrogen bond formation between water molecules and the hydroxyl (–OH) groups of glycol ethers.[12–15] The increase in V_Φ^0 values with temperature can be attributed to several factors, such as the release of solvation molecules from the relaxed solvation layers of the solute into the mixture, thermal expansion, and the formation of hydrogen bonds. Additionally, as the molecular mass of the glycol ethers (BE < PE) increases, the solute–solvent interaction becomes stronger, as evidenced by the increase in V_Φ^0 values with longer solute chain lengths.[23–25]

The S_V^* values for each temperature and mannitol concentration are found to be positive, representing the semiempirical solute-solute interaction parameter. This indicates the presence of solute-solute interactions within the mixture, although their magnitude is smaller compared to the V_Φ^0 values. This suggests that solute–solvent interactions dominate over solute–solute interactions in the solution.[18,32–34]

TABLE VII. Values of partial molar volumes, (V_Φ^0), and experimental slopes, (S_V^*), of BE/PE in aqueous solution of D-mannitol at different temperatures (288.15–303.15 K); m_b is the concentration of D-mannitol, standard uncertainties, u, are $u(m) = 1$ %, $u(T) = 0.001$ K, $u(\rho) = 0.15$ kg·m^{-3}, u(v) = 1.0 m·s^{-1}, $u(V_\Phi^0) = \pm0.01\times10^6$ m^3·mol^{-1} and $u(S_V^*) = \pm0.03\times10^6$ m^3·kg·mol^{-2}

m_b mol·kg^{-1}	$V_\Phi^0\times10^6$ / m^3·mol^{-1}				$S_V^*\times10^6$ / m^3·kg·mol^{-2}			
	T / K							
	288.15	293.15	298.15	303.15	288.15	293.15	298.15	303.15
BE								
0.00	116.05 (±0.010)	116.18 (±0.012)	116.33 (±0.010)	116.43 (±0.010)	0.7484 (±0.032)	0.7634 (±0.037)	0.7975 (±0.046)	0.8437 (±0.032)
0.02	116.14 (±0.007)	116.28 (±0.011)	116.42 (±0.008)	116.53 (±0.003)	0.9783 (±0.021)	1.0266 (±0.034)	1.0059 (±0.024)	1.0332 (±0.011)
0.06	116.24 (±0.004)	116.36 (±0.003)	116.50 (±0.002)	116.62 (±0.008)	1.0179 (±0.014)	1.0176 (±0.008)	1.0511 (±0.008)	1.0490 (±0.025)
0.10	116.34 (±0.004)	116.46 (±0.006)	116.59 (±0.009)	116.71 (±0.002)	1.0176 (±0.014)	1.0304 (±0.020)	1.0553 (±0.028)	1.0310 (±0.006)
PE								
0.00	133.39 (±0.007)	133.48 (±0.009)	133.59 (±0.010)	133.68 (±0.012)	0.9026 (±0.023)	0.9587 (±0.028)	0.9370 (±0.031)	0.9800 (±0.038)
0.02	133.53 (±0.002)	133.61 (±0.002)	133.71 (±0.006)	133.79 (±0.004)	0.7092 (±0.008)	0.7259 (±0.008)	0.7682 (±0.018)	0.7679 (±0.013)

TABLE VII. Continued

m_b mol·kg^{-1}	$V_\Phi^0 \times 10^6$ / m^3·mol^{-1}				$S_V^* \times 10^6$ / m^3·kg·mol^{-2}			
	T / K							
	288.15	293.15	298.15	303.15	288.15	293.15	298.15	303.15
	PE							
0.06	133.62 (±0.010)	133.69 (±0.006)	133.78 (±0.003)	133.86 (±0.005)	0.9415 (±0.030)	0.9579 (±0.019)	0.9713 (±0.010)	0.9832 (±0.015)
0.10	133.73 (±0.002)	133.80 (±0.001)	133.88 (±0.003)	133.99 (±0.005)	0.8956 (±0.006)	0.9168 (±0.004)	0.9609 (±0.009)	0.9636 (±0.016)
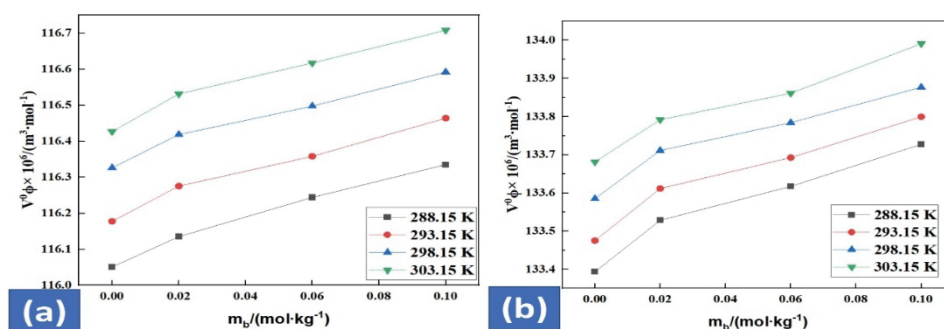
Fig. 6. Graphical illustration of partial molar volume (V_Φ^0) against the concentration of mannitol (m_b) at different temperatures: a) BE and b) PE (square, 288.15 K; circle, 293.15 K; triangle, 298.15 K; inverted triangle, 303.15 K).

Partial molar isentropic compressibility

The partial molar isentropic compressibility of liquid mixtures containing mannitol and glycol ethers is determined using as:

$$k_{\Phi,S} = K_{\Phi,S}^0 + S_k^* m_A \tag{5}$$

Table VIII presents the values of partial molar isentropic compressibility ($K_{\Phi,S}^0$) and experimental slope (S_k^*). In Fig. 7 the $K_{\Phi,S}^0$ values are represented graphically. These values are acquired by applying the method of least square fitting.

The $K_{\Phi,S}^0$ values are negative and decrease with increasing mannitol concentration and temperature. This trend implies the existence of strong interaction in water and glycol ethers in the mixture, causing some water molecules to be released into the bulk. The compressibility of water around glycol ethers is less at lower mannitol concentrations, but more at higher concentrations because of dominant interaction between mannitol and water, which dehydrates the glycol ethers molecules. The $K_{\Phi,S}^0$ values are affected by intermolecular interactions and is connected to the partial volume change of a solution. Ion dipole and hydrogen bonding occur, and are brought about by electrostatic forces between the polar group of mannitol, water and the ions of glycol ethers.[20–26] This shows that

the molecules in the solutions are tightly packed and well organized as the temperature drops, the strength of these connections increases, and partial molar compressibility values decrease. It showed that ions developed their structure-forming or structure-deforming behavior as a result of their strong interactions with water particles, such as H-bonding with water particles. Greater molecular interactions are present in the system with a lower compressibility value and *vice versa*.[40–43] According to the S_k^* values in the table, solute–solute interactions are minimal in a liquid mixture while they predominate in a solution.[39]

TABLE VIII. Values of Partial molar isentropic compressibility, ($K_{\Phi,S}^0$ / m^3·mol^{-1}· GPa^{-1}) and experimental slopes, ($S_k^* \times 10^6$ / kg·m^3·mol^{-2}· GPa^{-1}) of BE/PE in aqueous solution of D-mannitol at different temperatures; m_b is the concentration of D-mannitol, standard uncertainties, u, are $u(m)$ = 1 %, $u(T)$ = 0.001 K, $u(\rho)$ = 0.15 kg·m^{-3}, $u(v)$ = 1.0 m·s^{-1}, $u(K^0_{\Phi,S})$ = ±0.01×10^6 m^3·mol^{-1} and $u(S_k^*)$ = ±0.24×10^6 m^3·kg·mol^{-2}

| m_b mol·kg^{-1}	$K_{\Phi,S}^0$				S_k^*			
	T / K							
	288.15	293.15	298.15	303.15	288.15	293.15	298.15	303.15
	BE							
0.00	−46.03	−45.04	−44.24	−43.48	−0.9353	−0.9163	−0.9008	−0.8891
0.02	−45.84	−44.89	−44.05	−43.33	−0.9162	−0.8958	−0.8822	−0.8714
0.06	−45.60	−44.64	−43.82	−43.08	−0.8841	−0.8668	−0.8527	−0.8412
0.10	−45.39	−44.42	−43.57	−42.82	−0.8712	−0.8544	−0.8392	−0.8289
	PE							
0.00	−46.00	−45.01	−44.21	−43.45	−1.1271	−1.1058	−1.0907	−1.0772
0.02	−45.84	−44.89	−44.06	−43.33	−1.0338	−1.0141	−0.9998	−0.9899
0.06	−45.61	−44.64	−43.82	−43.08	−0.9959	−0.9782	−0.9650	−0.9538
0.10	−45.40	−44.43	−43.57	−42.82	−0.9705	−0.9542	−0.9395	−0.9274
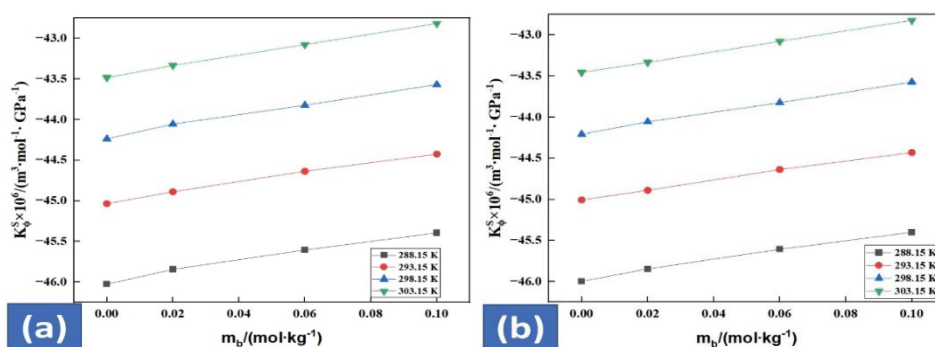
Fig. 7. Graphical illustration of partial molar isentropic compressibility ($K_{\Phi,S}^0$) against the concentration of mannitol (m_b) at different temperatures: a) BE and b) PE (square, 288.15 K; circle, 293.15 K; triangle, 298.15 K; inverted triangle, 303.15 K).

CONCLUSION

The Anton-Paar DSA 5000 M was employed in the experimental setup to measure both the density and speed of sound. This data was pivotal in exploring the volumetric and acoustic properties of the solutions. The substances under investigation, glycol ethers, and D-mannitol, have diverse applications in industries like pharmaceuticals, cosmetics, leather and food. Examining the mixture's thermodynamics allows us to understand the molecular interactions between these liquids. Using the DSA system is advantageous as it prevents structural deformations in glycol ethers within aqueous D-mannitol, avoiding potential errors from suspension formation. Analyzing the acoustical properties and their variations with different molar concentrations of D-mannitol provides crucial insights into the intermolecular forces in the mixtures. Measuring the speed of sound is an effective means to characterize the physicochemical behavior of D--mannitol, reflecting solute–solvent interactions that lead to attracttive forces contributing to structure formation. Additionally, interactions such as dipole–dipole, dipole–induced dipole and electrostatic forces enhance the structure-forming tendency in this medium. The data obtained from this study lays a solid foundation for future research aimed at refining our understanding of these molecular interactions. Further investigations could delve into optimizing the mixture's properties for specific industrial applications, thus contributing to advancements in various sectors.

SUPPLEMENTARY MATERIAL

Additional data and information are available electronically at the pages of journal website: https://www.shD-pub.org.rs/index.php/JSCS/article/view/12593, or from the corresponding author on request.

И З В О Д

ТЕРМОФИЗИЧКО ИСПИТИВАЊЕ ГЛИКОЛ-ЕТАРА У РАСТВОРИМА МАНИТОЛА НА РАЗЛИЧИТИМ ТЕМПЕРАТУРАМА

NABAPARNA CHAKRABORTY[1,2], PRIYA THAKUR[1], KAILASH CHANDRA JUGLAN[1] и ABRAR HUSSAIN SYED[3]

[1]*Department of Physics, Lovely Professional University, Phagwara, 144401, Punjab, India,* [2]*Central Instrumentation Facility, Research and Development Cell, Lovely Professional University, Phagwara, 144401, Punjab, India* и [3]*Research and Development, Saputo Dairy Australia, Freshwater Place, 3006, Victoria, Australia*

Ултразвучна анализа може бити од велике помоћи за разумевање молекуларне динамике и интеракција у течним системима. Применом Anton–Paar инструмента (DSA 5000 M), измерене су брзина звука и густина гликол-етара, као што су феноксиетанол (PE) и бутоксиетанол (BE), у растворима добро познатог шећерног алкохола (D-манитол), при различитим концентрацијама и 0,1 MPa, у опсегу температура 288,15–303,15

K. Израчунати су различити акустично–термодинамички параметри, укључујући при-видне моларне параметре, парцијалне моларне параметре и преносна моларна својства, коришћењем експериментално добијених вредности брзине и густине. Ове изведене величине су искоришћене за изражавање интеракција између растворених материја и растварача. Предмет истраживања је и склоност растворене супстанце да изгради или разори структуре у растварачу. Урађена је анализа интеракција између молекула у тернарној смеши d-манитола и гликол етара у воденој средини.

REFERENCES

1. M. S. Raman, M. Kesavan, K. Senthilkumar, V. Ponnuswamy, *J. Mol. Liq.* **202** (2015) 115 (https://doi.org/10.1016/j.molliq.2014.12.014)
2. S. Emiliani, M. V. Bergh, A. S. Vannin, J. Biranane, Y. Englert, *Hum. Reprod.* **15** (2000) 905 (https://doi.org/10.1093/humrep/15.4.905)
3. C. Zhu, X. Ren, Y. Ma, *J. Chem. Eng. Data* **62** (2017) 477 (https://doi.org/10.1021/acs.jced.6b00766)
4. N. Chakraborty, K. C. Juglan, H. Kumar, *J. Chem. Thermodyn.* **154** (2021) 106326 (https://doi.org/10.1016/j.jct.2020.106326)
5. A. Ali, P. Bidhuri, S. Uzair, *Indian J. Phys.* **88(7)** (2014) 715 (https://doi.org/10.1007/s12648-014-0461-2)
6. N. Chakraborty, K. C. Juglan, H. Kumar, *J. Mol. Liq.* **337** (2021) 116605 (https://doi.org/10.1016/j.molliq.2021.116605)
7. H. Kumar, M. Singla, R. Jindal, *Monatsh. Chem.* **145** (2014) 1063 (https://doi.org/10.1007/s00706-014-1183-z)
8. P. Pradhan, R.S. Sah, M. N. Roy, *J. Mol. Liq.* **144** (2009) 149 (https://doi.org/10.1016/j.molliq.2008.11.001)
9. S. K. Lomesh, M. Bala, D. Kumar, *J. Mol. Liq.* **289** (2019) 109479 (https://doi.org/10.1016/j.molliq.2018.08.034)
10. J. Wawer, J. Krakowiak, W. Grzybkowski, *J. Chem. Thermodyn.* **40** (2008) 1193 (https://doi.org/10.1016/j.jct.2008.04.008)
11. R. Rani, A. Kumar, T. Sharma, T. Sharma, R. K. Bamezai, *J. Chem. Thermodyn.* **135** (2019) 260 (https://doi.org/10.1016/j.jct.2019.03.039)
12. H. Zarei, S. M. Asl, *Fluid Phase Equilib.* **457** (2018) 52 (https://doi.org/10.1016/j.fluid.2017.10.027)
13. X. Jiang, C. Zhu, Y. Ma, *J. Chem. Eng. Data* **58** (2013) 2970 (https://doi.org/10.1021/je400395u)
14. N. G. Tsierkezos, I. E. Molinou, *J. Chem. Eng. Data* **43** (1998) 989 (https://doi.org/10.1021/je9800914)
15. I. Gheorghe, C. Stoicescu, F. Sirbu, *J. Mol. Liq.* **218** (2016) 515 (https://doi.org/10.1016/j.molliq.2016.02.033)
16. B. Sinha, A. Sarkar, P. K. Roy, D. Brahman, *Int. J. Thermophys.* **32** (2011) 2062 (https://doi.org/10.1007/s10765-011-1060-5)
17. M. Liu, L. L. Wang, G. Q. L. N. Dong, D. Z. Sun, L. Y. Zhu, Y. Y. Di, *J. Chem. Thermodyn.* **43** (2011) 983 (https://doi.org/10.1016/j.jct.2011.02.005)
18. M. Scognamiglio, L. Jones, C. S. Letizia, A. M. Api, *Food Chem. Toxicol.* **50** (2012) 244 (https://doi.org/10.1016/j.fct.2011.10.030)
19. I. Lowe, J. Southern, *Lett. App. Microbiol.* **18** (1994) 115 (https://doi.org/10.1111/j.1472-765X.1994.tb00820.x)

20. M. S. Raman, G. Amrithaganesan, *Indian J. Phys.* **78**(12) (2004) 1329
21. D. Chawla, N. Chakraborty, K. C. Juglan, H. Kumar, *Chem. Papers* **75** (2021) 1497 (https://doi.org/10.1007/s11696-020-01403-y)
22. P. K. Banipal, S. Arti, T. S. Banipal. *J Chem. Eng. Data* **60** (2015) 1023 (https://doi.org/10.1021/je500886a)
23. I. Mozo, I. G. de la Fuente, J. A. Gonzalez, J. C. Cobos, N. Riesco, *J. Chem. Eng. Data* **53** (2008) 1404 (https://doi.org/10.1021/je8000975)
24. H. Makhlauf, N. Munoz-Rujas, F. Aguilar, B. Belhachemi, E. A. Montero, I. Bahadur, L. Negadi, *J Chem Thermodyn.* **128** (2019) 394 (https://doi.org/10.1016/j.jct.2018.08.029)
25. X. U. Wang, R. Fu, Y. Gua, L. Rusin, *J. Mol. Liq.* **197** (2014) 73 (https://doi.org/10.1016/j.molliq.2014.04.028)
26. J. G. Kirkwood, *Chem. Rev.* **24** (1939) 233 (https://doi.org/10.1021/cr60078a004)
27. Z. Yan, J. J. Wang, H. Zheng, D. Liu, *J. Solut. Chem.* **27** (1998) 473 (https://doi.org/10.1023/A:1022608906767)
28. H. L. Friedman, C. Krishnan, *J. Solut. Chem.* **2** (1973) 119 (https://doi.org/10.1007/BF00651969)
29. S. Li, W. Sang, R. Lin, *J. Chem. Thermodyn.* **34** (2002) 1761 (https://doi.org/10.1016/S0021-9614(02)00125-8)
30. A. Salabat, L. Shamshiri, F. Sahrakr, *J. Mol. Liq.* **118** (2005) 67 (https://doi.org/10.1016/j.molliq.2004.07.014)
31. A. K. Mishra, J. C. Ahluwalia, *J. Phys. Chem.* **88** (1984) 86 (https://doi.org/10.1021/j150645a021)
32. L. G. Hepler, *Can. J Chem.* **47** (1969) 4613 (https://doi.org/10.1139/v69-762)
33. B. Naseem, I. Arif, M. A. Jamal, *Arab. J. Chem.* **14** (2021) 103405 (https://doi.org/10.1016/j.arabjc.2021.103405)
34. A. K. Nain, R. Pal, *J. Chem. Thermodyn.* **60** (2013) 98 (https://doi.org/10.1016/j.jct.2013.01.008)
35. R. A. Miranda- Quintana, J. Smiatek, *ChemPhysChem* **21** (2020) 2605 (https://doi.org/10.1002/cphc.202000644)
36. Z. Yan, X. Wen, Y. Kang, S. Zhang, S. Wu, *J. Chem. Thermodyn.* **93** (2016) 172 (https://doi.org/10.1016/j.jct.2015.10.004)
37. F. J. Millero, in *Water and Aqueous Solutions: Structure, Thermodynamics, and Transport Processes*, R. A. Horne, Ed., Wiley, New York, 1972
38. W. G. McMillan, Jr., J. E. Mayer, *J. Chem. Phys.* **13** (1945) 276 (https://doi.org/10.1063/1.1724036)
39. C. V. Krishnan, H. L. Friedman, *J. Solut. Chem.* **2** (1973) 37 (https://doi.org/10.1007/BF00645870)
40. F. Franks, M. Pedley, D. S. Reid, *J. Chem. Soc., Faraday Trans. 1* **72** (1976) 359 (https://doi.org/10.1039/F19767200359)
41. N. Chakraborty, K. C. Juglan, H. Kumar, *J. Chem. Thermodyn.* **163** (2021) 106584 (https://doi.org/10.1016/j.jct.2021.106584)
42. R. K. Wadi, P. Ramasami, *J. Chem. Soc., Faraday Trans.* **93** (1997) 243 (https://doi.org/10.1039/A604650I)
43. N. Chakraborty, P. Thakur, K. C. Juglan, *E3S Web Conf.* **453** (2023) 01051 (https://doi.org/10.1051/e3sconf/202345301051).